Electronic Supplementary Material (ESI) for Soft Matter.

Supplementary Material for: Universal scaling of the diffusivity of dendrimers in a semidilute solution of linear polymers

Silpa Mariya,[1,2,3,a)] Jeremy J. Barr,[4,b)] P. Sunthar,[2,c)] and J. Ravi Prakash[3,d)]
[1)] *IITB-Monash Research Academy, Indian Institute of Technology Bombay, Mumbai, 400076, India.*
[2)] *Department of Chemical Engineering, Indian Institute of Technology Bombay, Mumbai, 400076, India.*
[3)] *Department of Chemical Engineering, Monash University, Melbourne, VIC 3800, Australia*
[4)] *School of Biological Sciences, Monash University, Clayton, VIC 3800, Australia.*

(Dated: 4 December 2023)

[a)]Electronic mail: silpa.mariya@monash.edu
[b)]Electronic mail: jeremy.barr@monash.edu
[c)]Electronic mail: p.sunthar@iitb.ac.in
[d)]Electronic mail: ravi.jagadeeshan@monash.edu

SI. RADIUS OF GYRATION VERSUS NUMBER OF BEADS FOR VARIOUS TOPOLOGIES

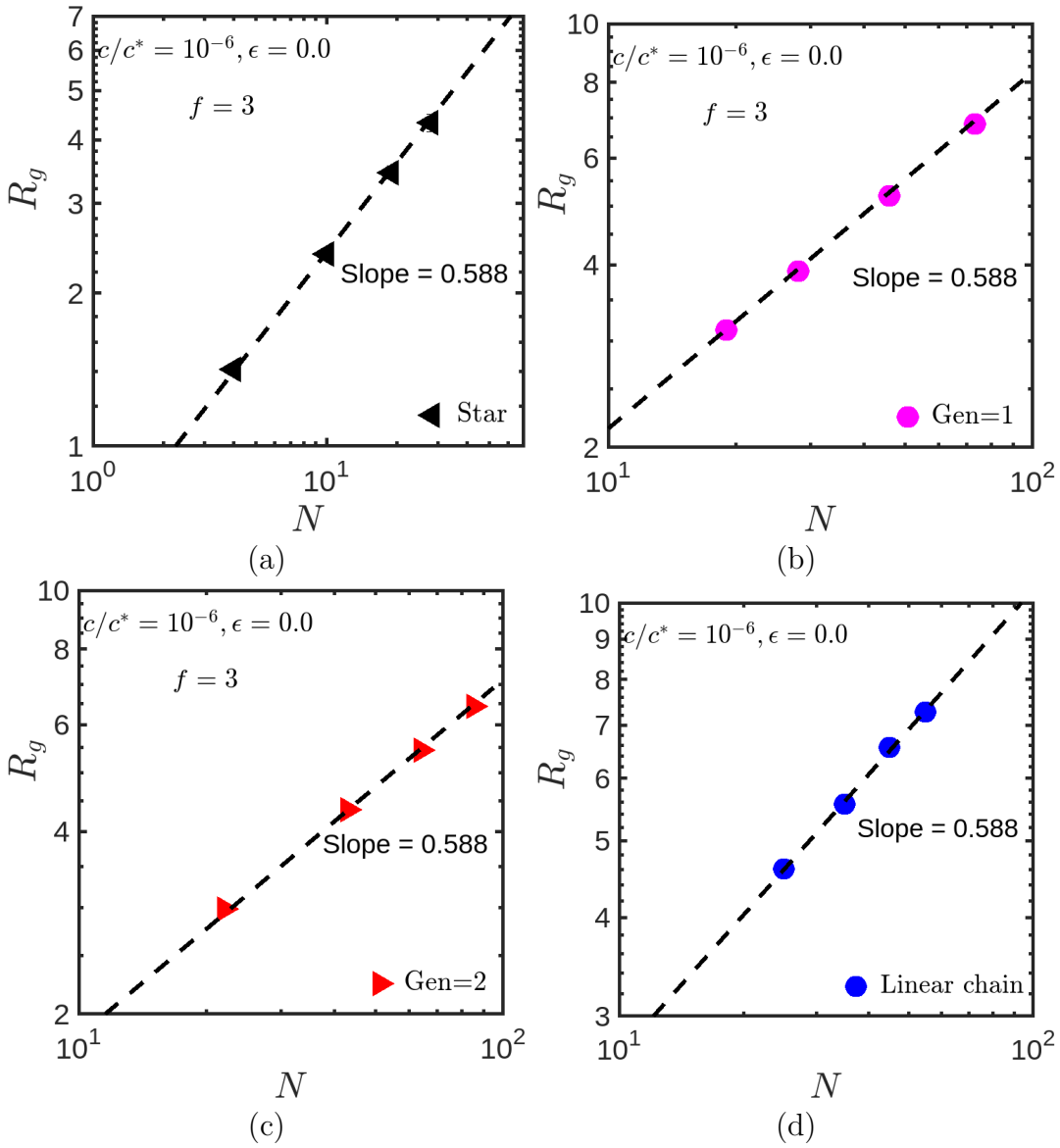

FIG. S1. (Color online) Radius of gyration versus number of beads per molecule (a) Star polymers with functionality 3. (b) Generation 1 dendrimer with functionality 3. (c) Generation 2 dendrimer with functionality 3. (d) Linear chains. The dashed lines are the scaling law given by eqns (S1) and (S2)

.

In order to determine the dendrimer parameters and length of linear chains in the solution, we used their respective radius of gyration versus number of beads per molecule plots. In Fig S1 (a),(b) and (c), the functionality (f) and generation number (g) of the dendrimer is fixed and number of beads is varied by changing the spacer length (s). Linear chains and dendrimers follow the scaling law given below:

$$R_{g0}^{\mathrm{lc}} = a^{\mathrm{lc}} \left(N_b^{\mathrm{lc}}\right)^{\nu} \tag{S1}$$

$$R_{g0}^{\mathrm{d}} = a^{\mathrm{d}} \left(N_b^{\mathrm{d}}\right)^{\nu} \tag{S2}$$

Here ν is the Flory exponent, $\nu = 0.588$. This information is used to construct Table 1 in the main text, for the various systems we have studied.

SII. SIZE REGIMES

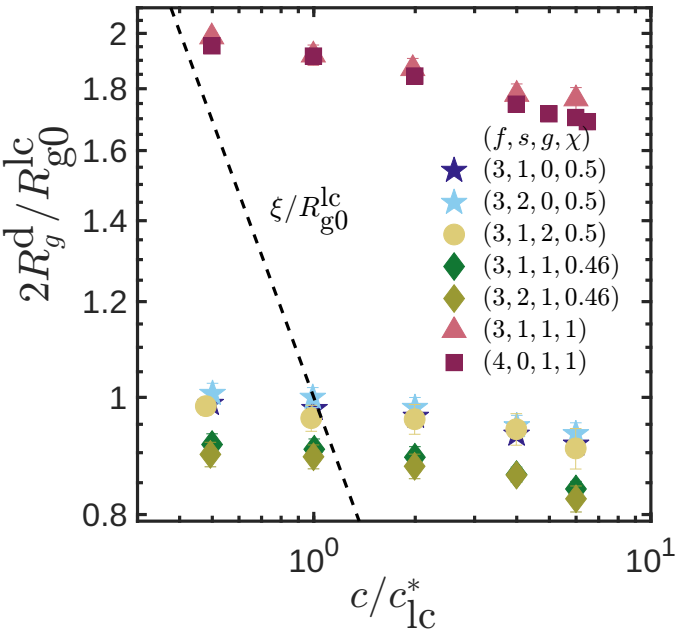

FIG. S2. (Color online) Size regimes based on relative sizes of polymers and correlation length of the solution. The dendrimer architecture is included in the order (f, s, g, χ). The y-axis is the ratio between the size of the dendrimer and the radius of gyration of the linear chain in the dilute limit in each simulation system. The dashed line represents the scaling of ξ with concentration given by eqn (S3).

The correlation length of the solution is given by[1],

$$\xi = R_{\rm g0}^{\rm lc} \left(\frac{c}{c^*_{\rm lc}} \right)^{\frac{-\nu}{(3\nu-1)}} \tag{S3}$$

where ν is the Flory exponent, assumed here to be equal to 0.588. At small concentrations, the size of the dendrimer is smaller than ξ (Regime-1). The correlation length decreases with concentration and beyond a certain concentration, the dendrimer is larger than ξ (Regime-2). Fig. S2 shows these regimes based on the relative size of dendrimers and the correlation length of the solution. The lengthscales are normalized with the radius of gyration of linear chains in the dilute limit to show the collapse of dendrimers with the same χ value.

SIII. DISTRIBUTION OF RADIUS OF GYRATION

Dendrimers are soft colloids and can have shape and size fluctuations based on the forces experienced by each of its constituent beads. This is evident from the distribution of its radius of gyration, $\psi(R_g^d)$. It is calculated by obtaining R_g^d from many trajectories at different instances in time and binning them. The variance of the distribution of R_g^d gives a measure of the size fluctuations. It is clear from Fig. S3(a) that increasing functionality reduces the softness of dendrimers resulting in lesser fluctuations. The $f = 4$ dendrimer has a significant decrease in

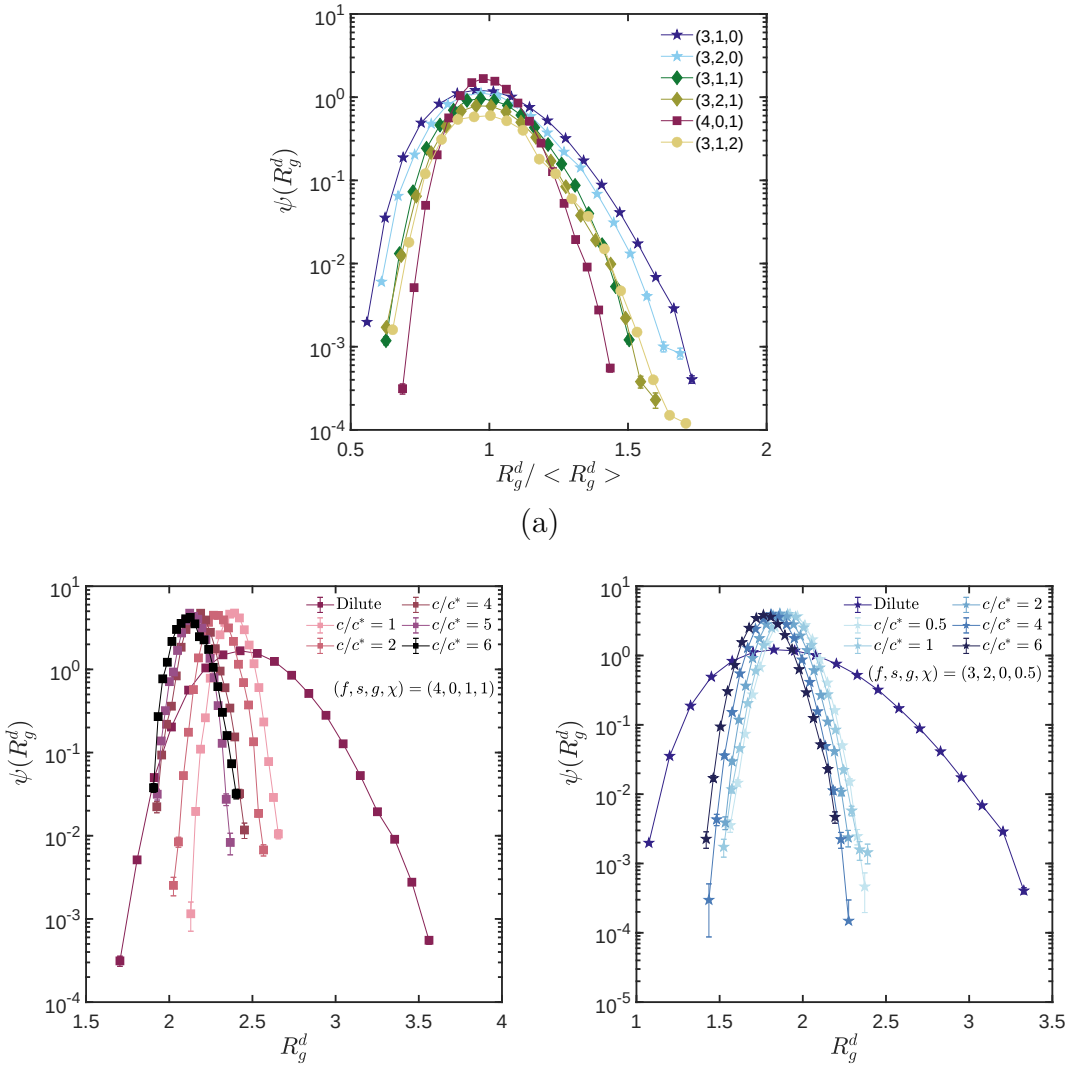

FIG. S3. (Color online) Distribution function of the radius of gyration of dendrimers (a) Dendrimers of different architectures in dilute solution. The dendrimer architecture is included in the order (f, s, g). Note that the x-axis is the normalised radius of gyration. (b) Effect of concentration on the size fluctuation of $(f, s, g, \chi) = (4, 0, 1, 1)$ dendrimers. (c) Effect of concentration on the size fluctuation of $(f, s, g, \chi) = (3, 1, 0, 0.5)$ dendrimers.

variance compared to the $f = 3$ dendrimers, especially the $(f, s, g) = (3, 1, 1)$ that has a similar number of beads per molecule to that of the $f = 4$ dendrimer. The fluctuations decrease at higher concentrations, but the distribution is similar at all concentrations irrespective of the architecture (shown in Fig. S3(b)).

SIV. ASPHERICITY

The asphericity B of a molecule is defined as[2–4]:

$$B = \langle \lambda_3^2 \rangle - \frac{1}{2} \left[\langle \lambda_1^2 \rangle + \langle \lambda_2^2 \rangle \right] \tag{S4}$$

Molecules with tetrahedral or greater symmetry have $B = 0$, otherwise $B > 0$. In Fig. S4(a), the

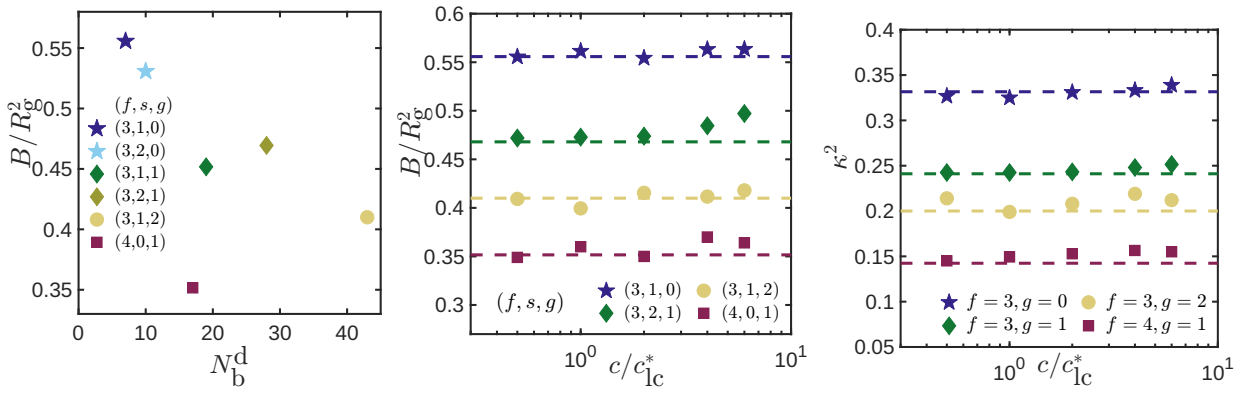

(a) (b) (c)

FIG. S4. (Color online) Effect of architecture and solution concentration on the shape of dendrimers. (a) Asphericity of dendrimers of different architectures in dilute solution as a function of the number of beads in a dendrimer molecule. The symbols represent dendrimer topology given by the combination f, s, g. (b) Effect of concentration of the solution on asphericity of dendrimers. All $f = 3$ architectures considered have one spacer bead ($s = 1$). The dashed lines are the asphericity in the dilute solution given in (a). (c) Effect of concentration of the solution on relative shape anisotropy of dendrimers. The dashed lines are the κ^2 in the dilute solution given in Fig.6(a) of the main text.

asphericity of dendrimers of different architectures in dilute solution, calculated using eqn (S4), is plotted as a function of the number of beads per molecule. In a dilute solution, an increase in generation number decreases B, implying a more spherically symmetric arrangement of beads within the molecule. The functionality four dendrimer has the lowest B value. A similar trend is observed in the case of the relative shape anisotropy. The concentration of the solution seems to not affect the asphericity and shape anisotropy of dendrimer molecules as seen in Fig. S4(b) and (c).

SV. BEAD DENSITY DISTRIBUTION

The linear bead density distribution along the 3 axes of the gyration tensor of $(f, s, g) = (3, 1, 1)$ dendrimer in dilute solution is shown in Fig. S5(a). The characteristic features of the distribution are observed along the major axis while it is Gaussian-like along the minor axes.

An alternative estimate of the internal density can also be obtained by counting the number of beads within concentric shells of constant thickness Δr starting from the centre of mass of the molecule. The volumetric bead density is given by:

$$\rho_{\mathrm{V}}(r) = \frac{n_{\mathrm{b}}(r + \Delta r) - n_{\mathrm{b}}(r)}{\Delta \mathrm{V}} \tag{S5}$$

where $n_{\mathrm{b}}(r)$ is the number of beads of a molecule in a sphere of radius r, ΔV is the volume of a spherical shell of thickness Δr given by $\frac{4}{3}\pi(r + \Delta r)^3 - \frac{4}{3}\pi r^3$. In Fig. S5(b), the volumetric bead densities in concentric shells starting from the centre of the molecule have been plotted for dendrimers in dilute solution. The density is maximum at the centre for all dendrimer architectures, which drops monotonically towards the periphery of the molecule. It is important to note that the dendrimers with a higher number of beads have lower core volumetric density. This might be because of the higher effective repulsion the individual beads near the centre feel, causing them to occupy regions towards the periphery. The $f = 3, s = 1, g = 1$ molecule in theta solvent has a significantly higher density at the core due to its collapsed state. In semidilute solution, the dendrimer volumetric bead density transitions from that in dilute solution to theta

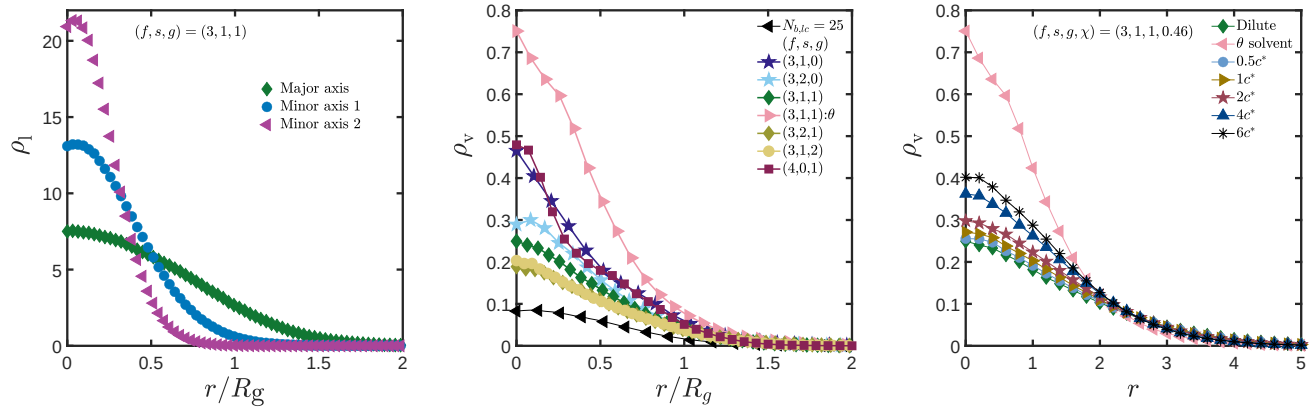

(a) (b)

FIG. S5. (Color online) Bead density distribution (a) Linear bead density distribution along the 3 axes for a $f = 3, s = 1, g = 1$ dendrimer in athermal solvent condition. (b) Effect of architecture on the volumetric bead densities of dendrimers in dilute solution. Black triangles represent linear chain with 25 beads and dendrimers are represented using the combination f, s, g. (c) Effect of concentration on the volumetric bead density distribution of $f = 3, s = 1, g = 1$ dendrimer in a semidilute solution of linear chains with $\chi = 0.46$. Pink triangles in both figures represent $f = 3, s = 1, g = 1$ dendrimer in theta solvent conditions.

solvent conditions as solution concentration increases (shown in Fig. S5(c)). This is consistent with the observations of linear bead density along the major axis and can be attributed to the onset of screening of EV at higher concentrations.

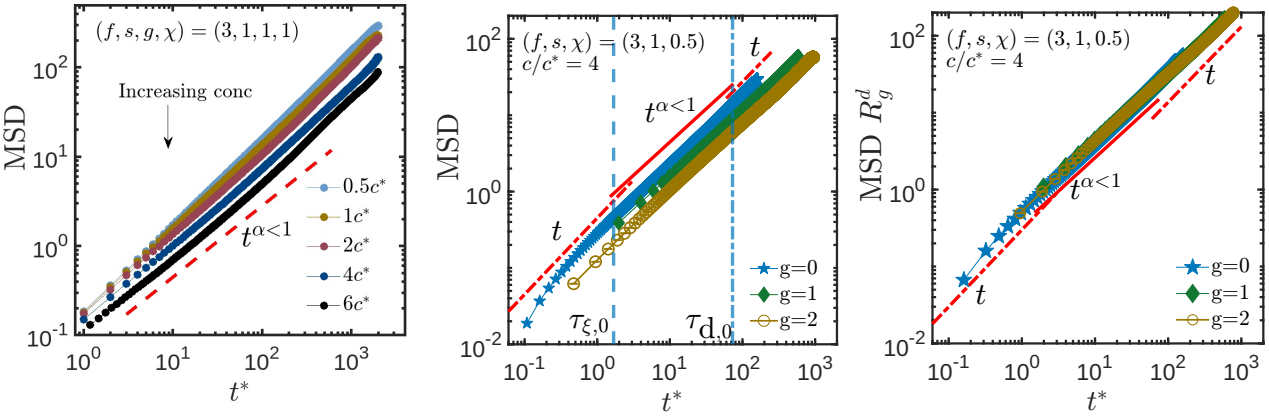

(a) (b) (c)

FIG. S6. (Color online) Mean squared displacement of dendrimers as a function of time (a) Effect of solution concentration on the mean squared displacement of generation one ($g = 1$) dendrimers with functionality $f = 3$ and one spacer bead ($s = 1$) in a solution of linear chains with 43 beads ($N_b^{lc} = 43$). The size ratio between the dendrimers and linear chains is 0.46 ($\chi = 0.46$). (b) Effect of generation number of dendrimers on its mean squared displacement. The concentration is $4c^*$ and dendrimer parameters are $f = 3, s = 1, \chi = 0.5$. The vertical dashed and dashed-dotted lines are τ_ξ and τ_d for the generation zero dendrimer respectively. (c) Collapse of mean squared displacement of dendrimers of different architectures considered in (b).

SVI. MEAN SQUARED DISPLACEMENT

The effect of solution concentration on the mean squared displacement of dendrimers is shown in Fig. S6(a). Subdiffusion is completely absent at low concentrations because the dendrimer size is much smaller than the solution correlation length. As concentration increases, due to the interaction between dendrimer molecules and the increased number of linear chains, a subdiffusive period exists ($\tau_\xi < t < \tau_d$) and the mean squared displacement of dendrimers decreases. Thus, with increased concentration, the dendrimers become less diffusive due to hindered motion. The values of τ_ξ and τ_ξ changes with concentration as reported in Tables S1, S2 and S3. Table S1 contains the values of τ_ξ and Table S2 contains the values of τ_d for all $f = 3$ dendrimers at all concentrations. Table S3 contains τ_ξ and τ_d for the $f = 4, g = 1$ dendrimer. When the size of the dendrimer is smaller than the correlation length (ξ) of the solution, it exhibits normal diffusion at all time scales and the concept of the time scales τ_ξ and τ_d does not exist.

TABLE S1. The time scale τ_ξ (given by eqn 17 in the main text) for the various architectures at different concentrations.

(χ, f, s, g)	c/c^*				
	0.5	1	2	4	6
$(0.5, 3, 1, 0)$	–	–	8.4	1.68	1.1
$(0.5, 3, 2, 0)$	–	–	14.6	2.9	1.9
$(0.46, 3, 1, 1)$	–	–	33.5	7.02	4.7
$(0.46, 3, 2, 1)$	–	–	65.1	13.62	9.1
$(0.5, 3, 1, 2)$	–	–	82.5	17.34	6.96
$(1.0, 3, 1, 1)$	–	18.3	3.96	0.96	0.6

TABLE S2. The time scale τ_d (defined by eqn 18 in the main text) for the various architectures at different concentrations.

(χ, f, s, g)	c/c^*				
	0.5	1	2	4	6
$(0.5, 3, 1, 0)$	–	–	48.9	72.9	93.1
$(0.5, 3, 2, 0)$	–	–	92.1	136.3	175.6
$(0.46, 3, 1, 1)$	–	–	168	248.6	302.4
$(0.46, 3, 2, 1)$	–	–	304.3	480.3	543.3
$(0.5, 3, 1, 2)$	–	–	556.8	864	1017.6
$(1.0, 3, 1, 1)$	–	245.7	369.6	517.4	676.8

The size of dendrimers varies with their generation number. Therefore, at a constant concentration, f and s, a generation 2 dendrimer will experience more hindrance to its motion compared to a simple star polymer ($g = 0$), causing the former to diffuse slower than the latter as shown in Fig. S6(b). The mean squared displacement of dendrimers is given by $\text{MSD} = 6\,D\,t$, where D is the diffusivity. The Stokes-Einstein relation for a particle of radius R is $D = k_B T/6\pi\eta R$. Therefore, $\text{MSD} \approx k_B T t/\eta R$, and $\text{MSD}\,R \approx k_B T t/\eta$. Using this simple

TABLE S3. The time scales τ_ξ and τ_d (defined by eqns 17 and 18 in the main text) for the $(\chi, f, s, g) = (1, 4, 0, 1)$ dendrimer.

c/c^*	τ_ξ	τ_d
0.5	–	–
1.0	9.2	124.8
2.0	1.9	181.4
4.0	0.6	247.6
5.0	0.4	273.6
6.0	0.3	305.2
6.5	0.2	313.9

scaling argument, we have collapsed MSD data for dendrimers of different generations as shown in Fig. S6(c).

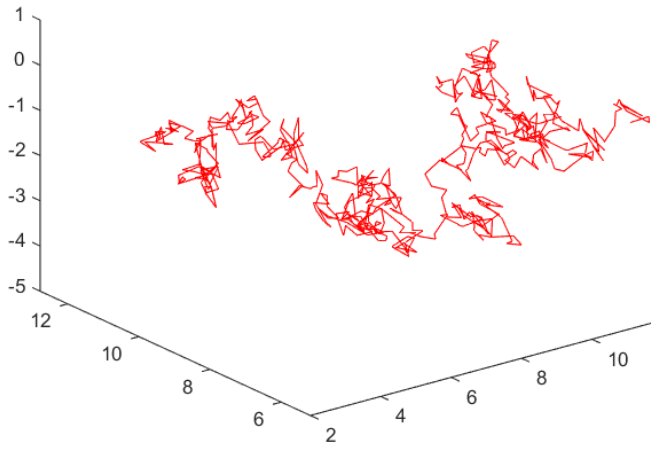

FIG. S7. (Color online) 3D plot of the movement of the centre of mass of the dendrimer. It is a $(f, s, g, \chi) = (3, 1, 1, 1)$ dendrimer molecule at $c/c^* = 6$ in the presence of hydrodynamic interactions.

An examination of the position of the centre of mass of a dendrimer molecule in our simulations as a function of time shows that it does not have long waiting times or hopping motion (Fig. S7). Rather the molecule moves in space via smooth random movements even at high concentrations.

SVII. DIFFUSION EXPONENT AS A FUNCTION OF TIME

The subdiffusion exponent can also be obtained by taking instantaneous derivatives in the mean squared displacement as given below:

$$\alpha = \frac{d \log(\mathrm{MSD}(\tau))}{d \log \tau} \tag{S6}$$

Fig. S8(a) shows the diffusion exponents of $(f, s, g, \chi) = (3, 1, 1, 1)$ dendrimer as a function of time at $c/c^* = 1$. It is clear that the dendrimer becomes subdiffusive when $\tau_\xi < \tau < \tau_d$ with the value of α in the subdiffusive regime similar to that obtained from the time exponent in the mean squared displacement plots. It transitions to a diffusive regime beyond τ_d. Similar behaviour is observed for all concentrations as shown in Fig. S8(b).

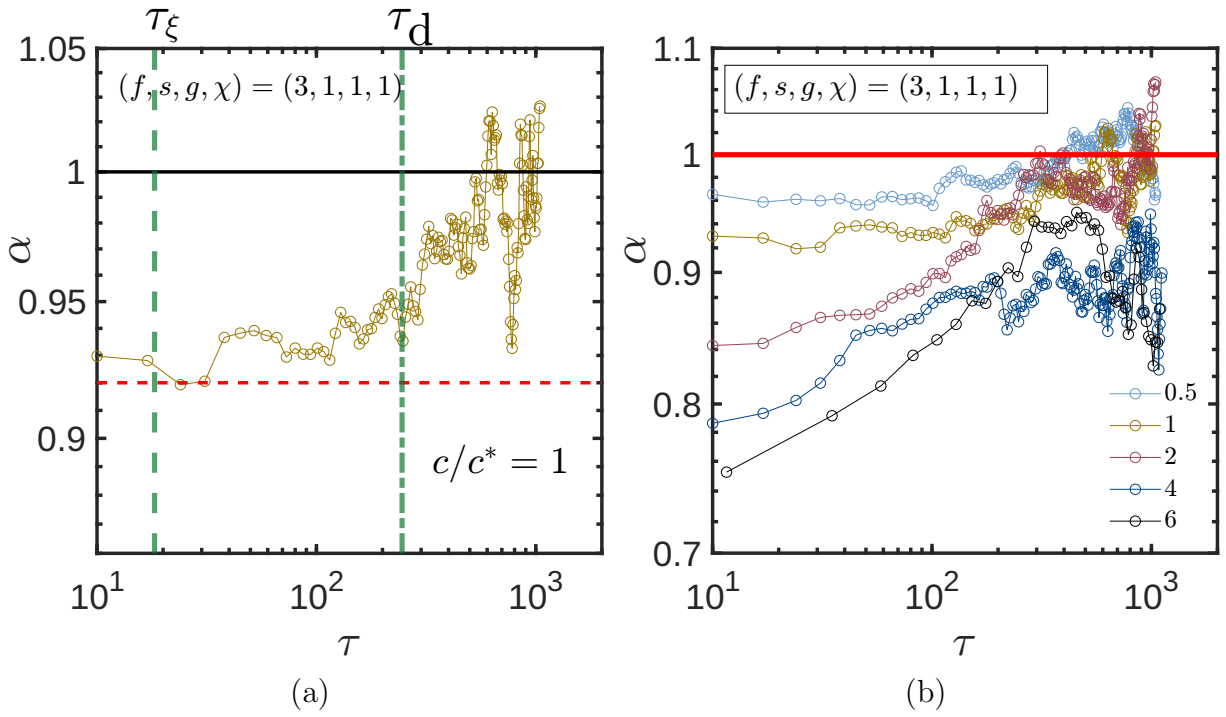

FIG. S8. (Color online) Diffusion exponent of $(f, s, g, \chi) = (3, 1, 1, 1)$ dendrimer as a function of time (a) The concentration considered is $c/c^* = 1$. Vertical lines represent τ_ξ (dashed) and τ_d (dashed-dotted) for $c/c^* = 1$. The horizontal dashed line is the value obtained from mean squared displacement versus time plots and the solid line is unity. (b) Diffusion exponent for different concentrations.

SVIII. VELOCITY FIELD DUE TO HYDRODYNAMIC INTERACTIONS

As pointed out in the manuscript, the subdiffusive motion of dendrimers is observed at intermediate times ($\tau_\xi < t < \tau_d$) which corresponds to the mean squared displacement of the dendrimer in the range $\xi <$ MSD $< 2R_g^d$. This suggests that on such time scales, the distance covered by a dendrimer is of the order of the cage size formed by polymer strands in the solution. To examine this closely, we have now computed the velocity fields within the solution due to hydrodynamic interactions as shown in Fig. S9. This velocity perturbation is obtained by calculating the product of the RPY tensor and the force exerted by each monomer at a point. Fig. S9 (a), (c) and (e) show the velocity field at lengthscales comparable to dendrimer size at different instances in time while Fig. S9 (b), (d) and (f) show the fields at large length scales corresponding to them. This enables us to see the effect of HI which we have observed in MSD plots. As is clear in the zoomed-in figures, each monomer on the dendrimer feels forces of different magnitudes and directions due to its location relative to the backflow. The net effect would be to randomize the direction of motion on small length and time scales, leading to slower diffusion. At longer times, $(t > \tau_d)$, the mean squared displacement of the dendrimer is much larger than its size. When observed from such large lengthscales, the entire molecule is like a single particle placed at its centre of mass with the orientation of individual beads being unimportant. The flow field set up due to HI seems to be in a particular direction and we would expect it to enhance diffusion. This explains the effect of HI at intermediate and long timescales.

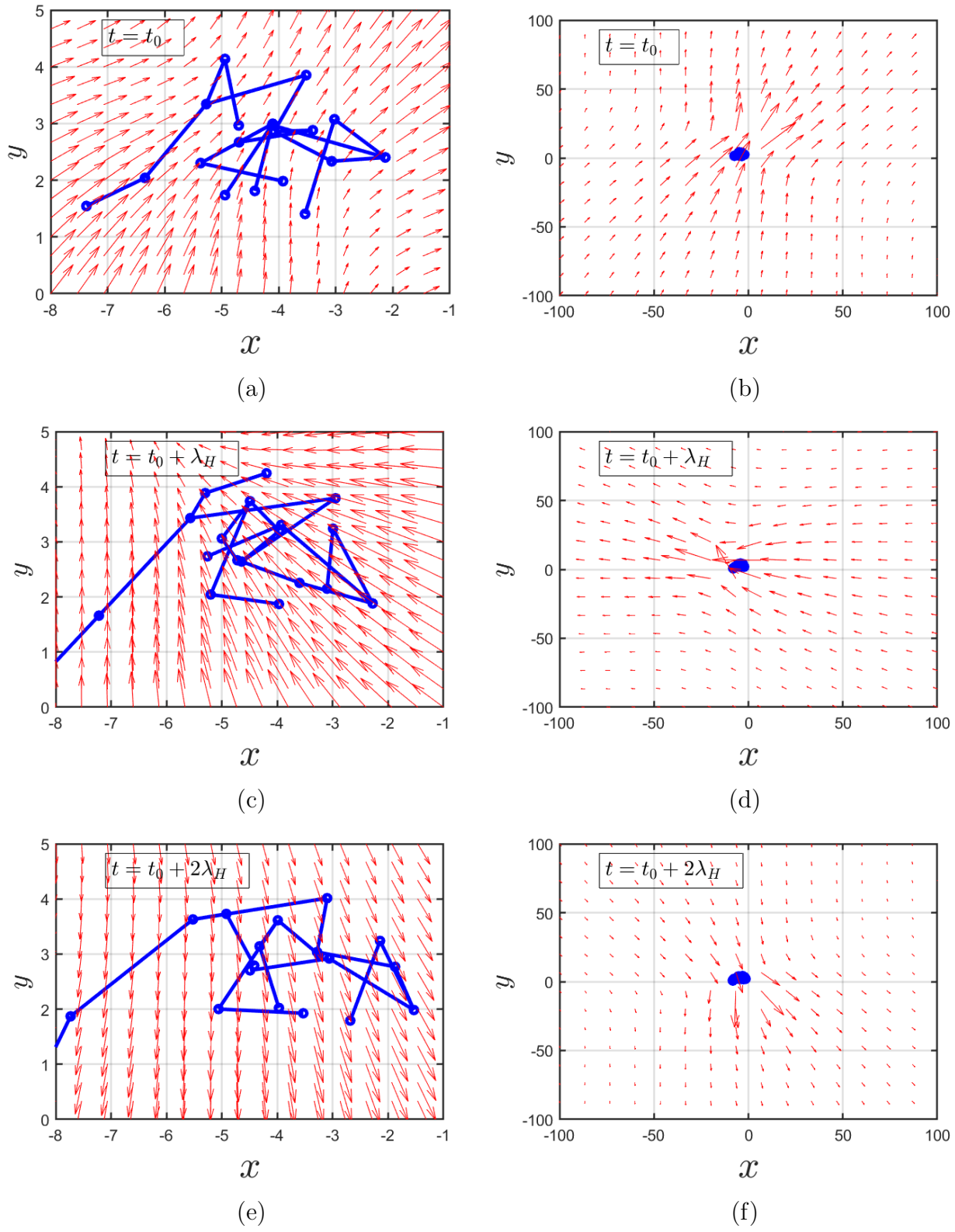

FIG. S9. (Color online) The flow field about a $(f, s, g, \chi) = (3, 1, 1, 1)$ dendrimer molecule at $c/c^* = 6$ in the presence of hydrodynamic interactions. The rows in the panel represent different instances in time. The first column (Fig (a), (c) and (e)) shows the velocity field about a dendrimer at a length scale of the order of the size of the dendrimer. The grid size is equal to the correlation length of the solution. The second column (Fig (b), (d) and (f)) shows the velocity field at a length scale much larger than the dendrimer size. The grid size is $\approx 50\xi$.

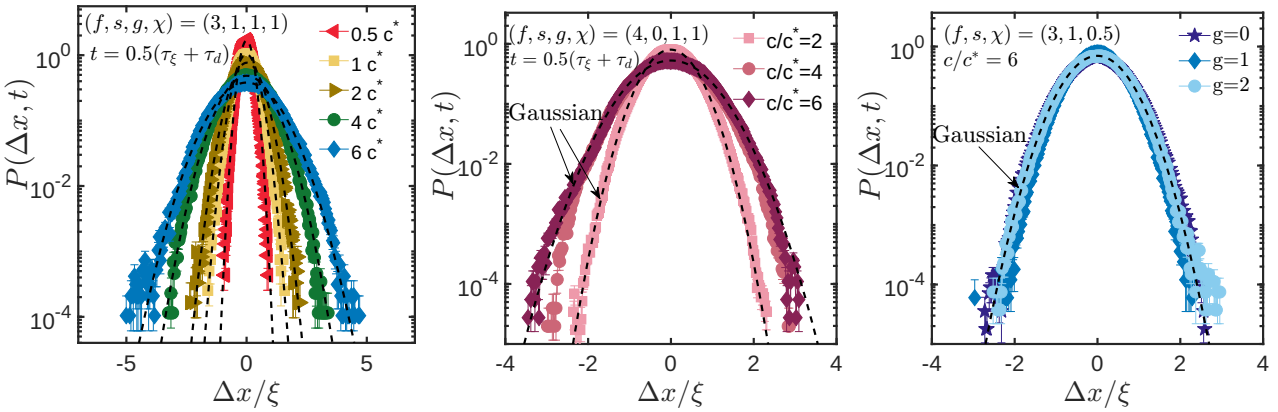

FIG. S10. (Color online) Probability distribution function of displacement for dendrimers. (a) Generation one dendrimer ($f=3, s=1, \chi=1$) in a semidilute solution of different concentrations in the subdiffusive regime $\tau_\xi > t > \tau_d$ (at $t=0.5(\tau_\xi+\tau_d)$). (b) PDD for $f=4$ dendrimer ($s=0, g=1, \chi=1$) in the subdiffusive regime at different concentrations (at $t=0.5(\tau_\xi+\tau_d)$). (c) Functionality three dendrimers of different generations in a semidilute solution of concentration $6c^*$ in the subdiffusive regime. The dashed lines in all figures are Gaussian fits to the data.

SIX. PROBABILITY DISTRIBUTION FUNCTIONS

The distribution of a $f=3, s=1, g=1$ at different concentrations (Fig. S10(a)) and dendrimers of different architectures (Fig. S10(c)) in the subdiffusive regime were also found to be Gaussian. Even the special case of a dendrimer with functionality $f=4$, which is a denser molecule, does not exhibit a non-Gaussian behaviour at any of the concentrations in the subdiffusive regime (shown in Fig. S10(b)).

SX. COMPARISON WITH DIFFUSIVITY OF OTHER SOFT COLLOIDS

We compared the dynamics of polymer grafted nanoparticles (PGNP), also called hairy colloids, in a solution of free polymer from work done by Poling-Skutvik *et al.*[5] with our simulations. According to them, the normalised diffusivity for various PGNP-free polymer systems can be collapsed if the normalised concentration (c/c^*) of free polymers is scaled with the ratio $(M_{w,f}/M_{w,g})^{-1/8}$. In our system, the radius of gyration of dendrimers and linear chains in dilute solution are related by the following equation:

$$\chi = \frac{R_{g0}^{d}}{R_{g0}^{lc}} \tag{S7}$$

If $\beta = N_b^{d}/N_b^{lc}$, then using eqns (S1) and (S2),

$$\chi = \frac{a^{d}}{a^{lc}}\beta^{\nu} \tag{S8}$$

The overlap concentration of dendrimers is

$$c_d^* = \frac{N_b^{d}}{(4/3)\,\pi (R_{g0}^{d})^3} \tag{S9}$$

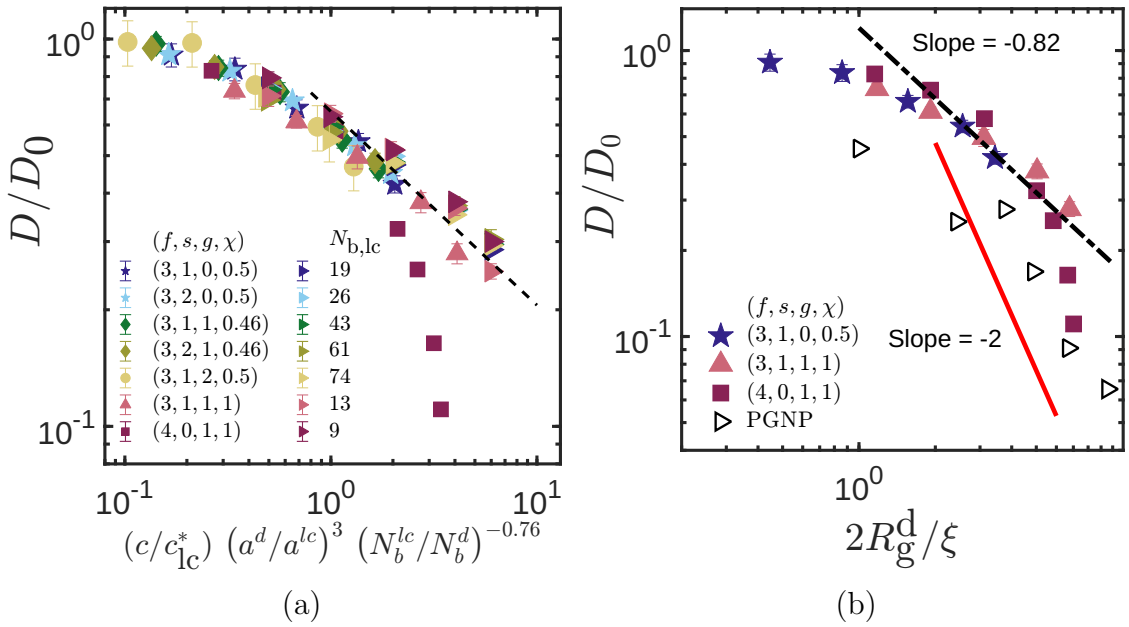

FIG. S11. (Color online) Effect of solution concentration and size of tracer on its diffusivity. (a)Normalised diffusivity of dendrimers as a function scaled c/c^*_{lc}. For comparison, data for linear chains is also included with c/c^*_{lc} in the x-axis. (b) Normalised diffusivity for dendrimers and PGNPs as a function of its size relative to the solution correlation length. The dashed line is the proposed scaling law for dendrimers and the solid line is the predictions of scaling theory.

Substituting eqns (S7) and (S8) in S9 gives

$$c^*_{\mathrm{d}} = c^*_{\mathrm{lc}} \left(\frac{N_b^{\mathrm{d}}}{N_b^{\mathrm{lc}}}\right)^{1-3\nu} \left(\frac{a^{lc}}{a^d}\right)^3 \tag{S10}$$

Using eqn (S10), we have shown that dendrimer diffusivity for all architectures can be collapsed if we use c/c^*_{lc} scaled by $\left(N_{\mathrm{b}}^{\mathrm{lc}}/N_{\mathrm{b}}^{\mathrm{d}}\right)^{-0.76}$ instead of c/c^*_{d} (Fig.S11(a)). Fig . S11(b) shows the normalised diffusivity as a function of the size of the dendrimer or PGNP ($M_{w,f}$ = 15000kDa, $M_{w,g}$ = 355 kDa)[5] relative to the system correlation length. Clearly, PGNP does not follow the same scaling behaviour as our simulated dendrimers. Rather they follow the nanoparticle scaling at intermediate values of $2R/\xi$. PGNP can reduce its size with increasing concentration similar to dendrimers. However, due to the presence of the nanoparticle which occupies almost 25% of the internal space, there is a limit beyond which it cannot shrink. Therefore, PGNP becomes nanoparticle-like at higher concentrations. Dendrimers reduce size with concentration and even start showing screening of excluded volume interactions as seen in the internal bead distribution plots.

SXI. SCALING LAW FOR DENDRIMER DIFFUSIVITY

Also, the correlation length (ξ) of the solution, radius of gyration of dendrimers ($R_{\mathrm{g}}^{\mathrm{d}}$) and linear chains ($R_{\mathrm{g}}^{\mathrm{lc}}$) in semidilute solutions depends on concentration as follows:

$$\xi = R_{\mathrm{g0}}^{\mathrm{lc}} \left(\frac{c}{c^*_{\mathrm{lc}}}\right)^{\mu} \tag{S11}$$

where $\mu = (-\nu)/(3\nu - 1)$.

$$R_{\mathrm{g}}^{\mathrm{d}} = R_{\mathrm{g0}}^{\mathrm{d}} \left(\frac{c}{c_{\mathrm{d}}^{*}} \right)^{\delta} \tag{S12}$$

where $\delta = (1 - 2\nu)/(2(3\nu - 1))$.

$$D^{\mathrm{d}} = D_{0}^{\mathrm{d}} \left(\frac{c}{c_{\mathrm{d}}^{*}} \right)^{\omega} \tag{S13}$$

where $\omega = (\nu - 1)/(3\nu - 1)$. Dividing eqn (S12) by eqn (S11),

$$\frac{2R_{\mathrm{g}}^{\mathrm{d}}}{\xi} = \frac{2R_{\mathrm{g0}}^{\mathrm{d}}}{R_{\mathrm{g0}}^{\mathrm{lc}}} \left(\frac{c}{c_{\mathrm{d}}^{*}} \right)^{\delta} \left(\frac{c}{c_{\mathrm{lc}}^{*}} \right)^{-\mu} \tag{S14}$$

We also have the overlap concentration of linear chains given by:

$$c_{\mathrm{lc}}^{*} = \frac{N_{\mathrm{b}}^{\mathrm{lc}}}{(4/3)\,\pi (R_{\mathrm{g0}}^{\mathrm{lc}})^{3}} \tag{S15}$$

Taking the ratio of equations (S9) and (S15) and substituting the values of χ and β give:

$$c_{\mathrm{lc}}^{*} = \left(\chi^{3}/\beta \right) c_{\mathrm{d}}^{*} \tag{S16}$$

Therefore,

$$\frac{2R_{\mathrm{g}}^{\mathrm{d}}}{\xi} = \frac{2\chi^{(1+3\mu)}}{\beta^{\mu}} \left(\frac{c}{c_{\mathrm{d}}^{*}} \right)^{\delta - \mu} \tag{S17}$$

$$\frac{c}{c_{\mathrm{d}}^{*}} = \left[\left(\frac{2R_{\mathrm{g}}^{\mathrm{d}}}{\xi} \right) \left(\frac{\beta^{\mu}}{2\chi^{(1+3\mu)}} \right) \right]^{1/(\delta - \mu)} \tag{S18}$$

From equation S13,

$$\frac{c}{c_{\mathrm{d}}^{*}} = \left[\frac{D^{\mathrm{d}}}{D_{0}^{\mathrm{d}}} \right]^{(1/\omega)} \tag{S19}$$

Equating equation S18 and S19, we get

$$\frac{D^{\mathrm{d}}}{D_{0}^{\mathrm{d}}} = \gamma \left(\frac{2R_{\mathrm{g}}^{\mathrm{d}}}{\xi} \right)^{\omega/(\delta - \mu)} \tag{S20}$$

where $\gamma = \left(\dfrac{\beta^{\mu}}{2\chi^{(1+3\mu)}} \right)^{\omega/(\delta - \mu)}$ and $\dfrac{\omega}{\delta - \mu} = 2(\nu - 1)$.

SXII. THE MITTAG-LEFFLER FUNCTION

The in-built MATLAB routine for evaluating the Mittag-Leffler function with two parameters was used for the fitting the modified Mittag-leffler function through the simulation data. The code can be found at: `https://www.mathworks.com/matlabcentral/fileexchange/`

8738-mittag-leffler-function.

SXIII. DIFFUSIVITY AS A FUNCTION OF RADIUS OF GYRATION

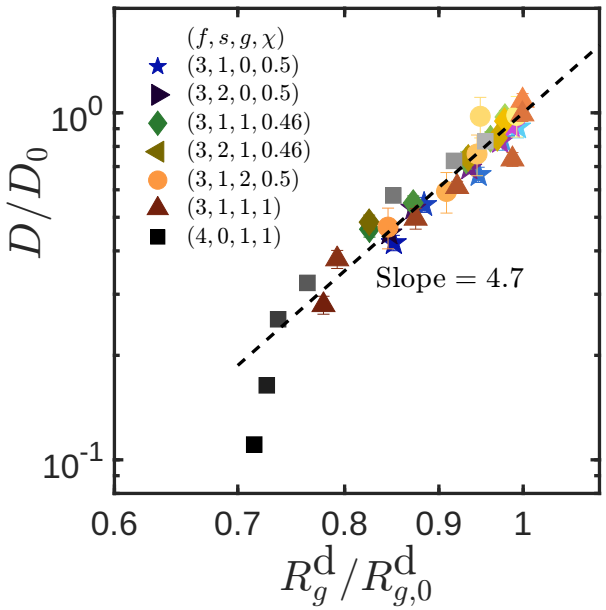

FIG. S12. (Color online) Normalised diffusivity as a function of the normalised radius of gyration for different dendrimer architectures. The dashed line has a slope equal to 4.7.

According to the predictions of the scaling theory[6], the long-time diffusivity of a nanoparticle in semidilute polymer solution is given by

$$D_{\mathrm{t}} \approx \frac{k_B T}{\eta_{\mathrm{eff}}(\tau_d) d} \tag{S21}$$

where $\eta_{\mathrm{eff}}(\tau_d) = \eta_s (d/\xi)^2$ is the effective viscosity experienced by a nanoparticle of size d in a solution with solvent viscosity η_s and correlation length ξ. On substituting this in eqn (S21), the result $D_{\mathrm{t}} \propto 1/d^3$ is obtained as pointed out by the reviewer. The size of a nanoparticle remains constant at all polymer concentrations. However, this is not true in the case of dendrimers. The radius of dendrimers decreases with concentration as follows:

$$R_{\mathrm{g}}^{\mathrm{d}} = R_{\mathrm{g0}}^{\mathrm{d}} \left(\frac{c}{c_{\mathrm{d}}^*} \right)^{\delta} \tag{S22}$$

where $\delta = (1 - 2\nu)/(2\,(3\nu - 1))$. Therefore,

$$\frac{c}{c_{\mathrm{d}}^*} = \left(\frac{R_{\mathrm{g}}^{\mathrm{d}}}{R_{\mathrm{g0}}^{\mathrm{d}}} \right)^{(1/\delta)} \tag{S23}$$

The diffusivity of most of the dendrimer architectures follows the scaling law for linear chains as given below:

$$D^{\mathrm{d}} = D_0^{\mathrm{d}} \left(\frac{c}{c_{\mathrm{d}}^*} \right)^{\omega} \tag{S24}$$

where $\omega = (\nu - 1)/(3\nu - 1)$. Substituting eqn (S23) in eqn (S24), we have

$$\frac{D^{\mathrm{d}}}{D_0^{\mathrm{d}}} = \left(\frac{R_{\mathrm{g}}^{\mathrm{d}}}{R_{\mathrm{g0}}^{\mathrm{d}}} \right)^{(\omega/\delta)} \tag{S25}$$

Substituting for $\nu = 0.588$ in athermal conditions, $\omega/\delta = 4.7$. Fig S12 shows the variation of normalised diffusivity as a function of normalised dendrimer size. All the dendrimer architectures, except the $f = 4$ dendrimer collapse to a universal curve. This shows that the diffusivity scales as $(R_g^d)^{4.7}$ instead of the -3 scaling of nanoparticles.

REFERENCES

[1]R. H. Colby and M. Rubinstein, New-York: Oxford University **100**, 274 (2003).
[2]D. N. Theodorou and U. W. Suter, Macromolecules **18**, 1206 (1985).
[3]M. Bishop and J. Michels, J. Chem. Phys. **85**, 5961 (1986).
[4]K. Kumari, B. Duenweg, R. Padinhateeri, and J. R. Prakash, Biophys. J. **118**, 2193 (2020).
[5]R. Poling-Skutvik, A. H. Slim, S. Narayanan, J. C. Conrad, and R. Krishnamoorti, ACS Macro Letters **8**, 917 (2019).
[6]L.-H. Cai, S. Panyukov, and M. Rubinstein, Macromolecules **44**, 7853 (2011).